ISSN 1028-334X, Doklady Earth Sciences, 2007, Vol. 414, No. 4, pp. 599–604. © Pleiades Publishing, Ltd., 2007.
Original Russian Text © A.B. Kuznetsov, M.T. Krupenin, I.M. Gorokhov, A.V. Maslov, G.V. Konstantinova, E.P. Kutyavin, 2007, published in Doklady Akademii Nauk, 2007, Vol. 414, No. 2, pp. 233–238.

GEOCHEMISTRY

Strontium Isotopic Composition of Lower Riphean Carbonate Rocks in the Magnesite-Bearing Satka Formation, Southern Urals

A. B. Kuznetsov[a], M. T. Krupenin[b], I. M. Gorokhov[a], Corresponding Member of the RAS A.V. Maslov[b], G. V. Konstantinova[a], and E. P. Kutyavin[a]

Received December 21, 2006

DOI: 10.1134/S1028334X07040241

Great interest in the genesis of stratiform deposits of sparry magnesite has been stimulated by a number of convergent attributes that admit a sedimentary, infiltration, hydrothermal metasomatic, and even metamorphic origin of magnesite bodies [1–4]. The analysis of Sr isotopic composition of magnesites and other carbonates is a tool that makes it possible to estimate the geochemical characteristics of the sedimentary medium and specific features of postsedimentary transformations of rocks. Despite long-term interest in the issue of magnesite formation, the Rb–Sr systematics of magnesite and host carbonate rocks has been considered only in a few publications, and all they deal with the Veitsch-type sparry magnesites hosted in the Paleozoic rocks of the Alpine Foldbelt [4, 5].

The large stratiform magnesite bodies known from the Lower Riphean Satka Formation in the Satka–Bakal ore district of the southern Urals [1, 6, 7] are similar to the Veitsch-type deposits in structural features. However, their Rb–Sr systematics has not been studied until now. The aim of the present communication is to fill this gap.

The terrigenous–carbonate Satka Formation (1700–3500 m) is exposed in the northern Bashkir anticlinorium as the middle unit of the Burzyan Group, a stratotype of the Lower Riphean [6]. The Satka Formation conformably overlies the fine-grained siliciclastic rocks of the Ai Formation and underlies the shales of the Bakal Formation. The Satka Formation is subdivided into five subformations (from bottom to top): lower Kusa shale–dolomite (700–800 m), upper Kusa limestone–dolomite (300–600 m), Polovinka shale (180–200 m), lower Satka shale–dolomite (200–300 m), and upper Satka carbonate (650–1200 m). The upper Satka subformation consists of three members: Kamennogorka shale–dolomite (80–200 m), Karagai dolomite–magnesite (500–750 m), and Kazym limestone (30–150 m). Stratiform bodies (20–60 m thick) of coarse-grained and pinolitic magnesites are hosted in thin-bedded and brecciated dolomites of the lower part of the Karagai member. Separate magnesite bodies extend for a few kilometers and make up a 12-km-long chain oriented conformably to the general trend of the Satka syncline (Fig. 1).

The timing of the Satka Formation is constrained by the U–Pb zircon age of volcanic rocks from the underlying Ai Formation (1615 ± 45 Ma [8]) and Pb–Pb age of limestones from the overlying Bakal Formation (1430 ± 30 Ma) [9]). The isochron U–Pb zircon age of nepheline syenites in the Berdyaush pluton, which intrudes magnesite bodies in the Satka district, indicates that the Satka magnesite is older than 1368 ± 6 Ma [10].

The genesis of Satka magnesite is considered within the framework of several alternative models suggesting different sources of Mg and mechanisms of ore deposition: (i) the hydrothermal metasomatic model that supposes a magmatic source of Mg [11], (ii) the metasomatic model that assumes a transfer of the finely dispersed sedimentary magnesite from host dolomites into orebodies along with basinal brines [1], and (iii) the sedimentary model that assumes the supply of Mg comes from hypothetical weathered crusts formed after basic rocks [2]. The recent REE systematics of carbonate rocks in the Satka district indicates the low-temperature metasomatic replacement of dolomites with magnesites [6, 7]. The correlation of Cl/Br and Na/Br ratios established by the study of fluid inclusions in magnesites and dolomites from the Satka ore field suggests the formation of magnesite bodies as a result of infiltration of evaporitic magnesian brines [12]. The presence of collapse-breccia in the magnesite-hosting dolomites

[a] *Institute of Precambrian Geology and Geochronology, Russian Academy of Sciences, nab. Makarova 2, St. Petersburg, 199034 Russia; e-mail: antonbor@ak9723.spb.edu*

[b] *Zavaritskii Institute of Geology and Geochemistry, Ural Division, Russian Academy of Sciences, Pochtovyi per. 7, Yekaterinburg, 620151 Russia*

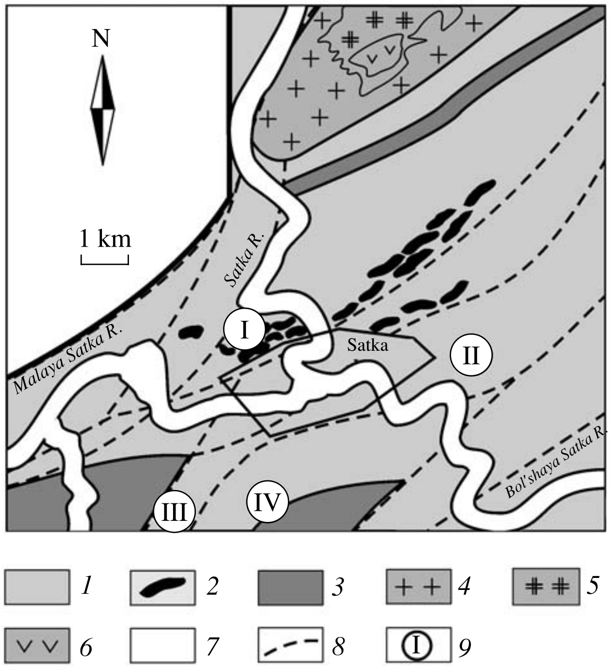

Fig. 1. Geological sketch map of the Satka district (modified after [1]) and sampling sites. (*1*) Carbonate rocks; (*2*) magnesite deposits; (*3*) shales and siltstones; (*4*) granites; (*5*) nepheline syenites; (*6*) gabbroic rocks; (*7*) Quaternary sediments; (*8*) faults; (*9*) location of samples (numerals in circles): (I) Magnesite Mine and Karagai open pit; (II) exposure at the Ufa–Chelyabinsk highway near the bridge across the Malaya Satka River; (III) exposure at the entry to the town of Satka; (IV) Mt. Kazym.

serves as indirect evidence for evaporite conditions of carbonate sedimentation. In the opinion of Krupenin [12], such breccia can be related to the dissolution of gypsum pockets and its replacement with coarse-crystalline dolomite.

In this communication, we present the first information on Rb–Sr systematics of the main carbonate lithotypes of the Satka Formation: limestones, dolomites, magnesites, and near-ore dolomites. Limestones were sampled in the Kazym member exposed on Mt. Kazym four kilometers south of the town of Satka (Fig. 2). The thickness of the Kazym member in this section does not exceed 30 m. Magnesite samples were taken from two ore beds (30–50 m thick) in the lower part of the Karagai member (Magnesite Mine). Three samples of near-ore dolomite were taken from the same locality at a distance of 1–2 m from magnesite bodies. One more sample of near-ore dolomite was taken 20 m below the magnesite body at the bottom of the Karagai open pit. Other dolomite samples characterize three levels of the Karagai member in marginal zones of the ore field: the middle level (exposure at the entry to the town of Satka), the upper level (exposure at the highway near the bridge across the Malaya Satka River), and the terminal level (10–20 m below the contact with the overlying Kazym limestone on Mt. Kazym). Dolomites from these levels are located at a distance of 100–110, 210–240, and 520–530 m, respectively, from magnesite bodies in the vertical direction.

The major oxide contents in the limestones, dolomites, and magnesites were determined by the chemical analysis; Mn and Fe contents in limestones and dolomites, by atomic absorption spectroscopy. The Rb–Sr systematics of limestones and dolomites located far from the ore field (hereafter, distal rocks) was studied with the method of sequential dissolution: preliminary treatment of a ground charge of rock with ammonium acetate solution (AA-fraction) and the subsequent dissolution of a residue in acetic acid (ACA-fraction) [13]. The data obtained for carbonate ACA-fractions of the studied samples are used in further discussion. The Rb–Sr systematics of magnesites and near-ore dolomites was studied in the bulk carbonate material after its dissolution in 2.5N HCl at 60°C. The Rb and Sr concentrations in all samples were determined with the isotope dilution technique [13]. The Sr isotopic composition was measured on a Finnigan MAT-261 multicollector mass spectrometer in the regime of simultaneous measurement of all isotope ion currents. During the period of data gathering, the average $^{87}Sr/^{86}Sr$ values in NIST SRM 987 and EN-1 standards normalized to $^{86}Sr/^{88}Sr = 0.1194$ were 0.71026 ± 0.00001 ($2\sigma_{aver}$, $n = 8$) and 0.70920 ± 0.00002 ($2\sigma_{aver}$, $n = 4$), respectively.

The studied limestones are represented by fine-crystalline calcite (< 0.3% Mg) with an insignificant admixture of quartz, illite, and chlorite (0.8–3.5%). The rocks are depleted in Mn (10–30 ppm) and Fe (250–1120 ppm), enriched in Sr (1140–2750 ppm), and characterized by a low $^{87}Sr/^{86}Sr = 0.70460–0.70520$ (table). The high Sr content in limestones suggests that the initial carbonate sediments contained aragonite. The positive correlation of $^{87}Sr/^{86}Sr$ with Mn/Sr (correlation coefficient $r = 0.87$) and Fe/Sr ($r = 0.86$) indicates the partial alteration of the Rb–Sr system in the calcareous sediment with the participation of atmospheric waters during the postsedimentary transformation of aragonite into calcite. Nevertheless, six limestone samples that contain more than 1500 ppm Sr satisfy the rigorous geochemical criterion of the Rb–Sr system retentivity (Mn/Sr < 0.2 and Fe/Sr < 5). It may be supposed that these samples are the least altered carbonate materials that retained the $^{87}Sr/^{86}Sr$ ratio of the sedimentation medium of the Satka time. The initial $^{87}Sr/^{86}Sr$ ratio in these samples (0.70460–0.70472, assuming their formation 1550 Ma ago) falls into the range of the published values (0.70456–0.70514) for the Early Riphean marine carbonate sediments from the Bakal Formation (southern Urals), the Kyutingda and Kotuikan formations (eastern Siberia), and the Belt Supergroup of North America (see the review and references in [9, 13]).

The distal dolomite samples are characterized by rather wide variations of the Mg/Ca ratio (0.59–0.64) and Sr content (24.6–62.8 ppm). The Satka dolomite is distinguished by a low Sr content from the Jatulian magnesite-bearing dolomite formed in evaporite lagoons and sabkha [14]. Quartz, illite, and chlorite admixtures in dolomite are commonly insignificant (0.7–5.3%) and as much as 15.5% in only one sample from the upper part of the Karagai member. The contents of Mn (45–160 ppm) and Fe (550–5750 ppm) and the measured $^{87}Sr/^{86}Sr$ ratio in dolomites (0.70743–0.73079) is higher than in limestones. These parameters have a positive correlation with the content of the terrigenous admixture, testifying to a partial exchange of minor elements and radiogenic ^{87}Sr between siliciclastic and carbonate constituents of dolomite, probably under conditions of a closed or semiclosed system.

The near-ore dolomites do not differ from dolomites of marginal zones in the Mg/Ca ratio (0.59–0.63) and average contents of Sr (45 ppm), Mn (150 ppm), and Fe (1680 ppm), but the measured $^{87}Sr/^{86}Sr$ ratio in the near-ore dolomites is appreciably lower (0.70659–0.70825). Upon approaching the magnesite body, this ratio increases from 0.70659 to 0.70825, varying within a narrow range of 0.70816 to 0.70822 in intervals between the near-ore dolomites. The share of the terrigenous admixture in the near-ore dolomites is low (1.0–3.8%).

The chemical composition of magnesites is close to the stoichiometric composition: Mg 27.4–28.7%, Ca content up to 0.3–0.8% (table). Quartz and Mg-chlorite impurities are insignificant (0.5–1.9%). In comparison with host dolomites, magnesites are enriched in Mn (220–330 ppm) and especially Fe (620–14500 ppm) and depleted in Sr (1.0–4.8 ppm). The positive correlation between Sr and Ca (r = 0.68) reflects isomorphic replacement of the Ca ion with Sr in magnesite. The $^{87}Sr/^{86}Sr$ ratio in the studied magnesite shows a negative correlation with the Fe content (r = –0.76) and does not depend on the amount of terrigenous admixture. The high $^{87}Sr/^{86}Sr$ ratio is inherent to both magnesite orebodies. However, this ratio decreases from inner to outer zones of the orebodies: from 0.71793 to 0.71425 in the first body and from 0.71935 to 0.71525 in the second body.

In contrast to aragonite and calcite, the structure of magnesium carbonates is favorable for the incorporation of elements with a relatively small ionic radius (e.g., Mn^{2+} and Fe^{2+}) and unfavorable for the incorporation of Sr^{2+}. Therefore, we can see a gradual gain of Mn and Fe and a significant loss of Sr in the calcite–dolomite–magnesite series. It is unlikely that carbonate material is enriched in Rb in the course of the mineral transformations mentioned above. This is indicated by similar Rb contents in the studied limestones, dolo-

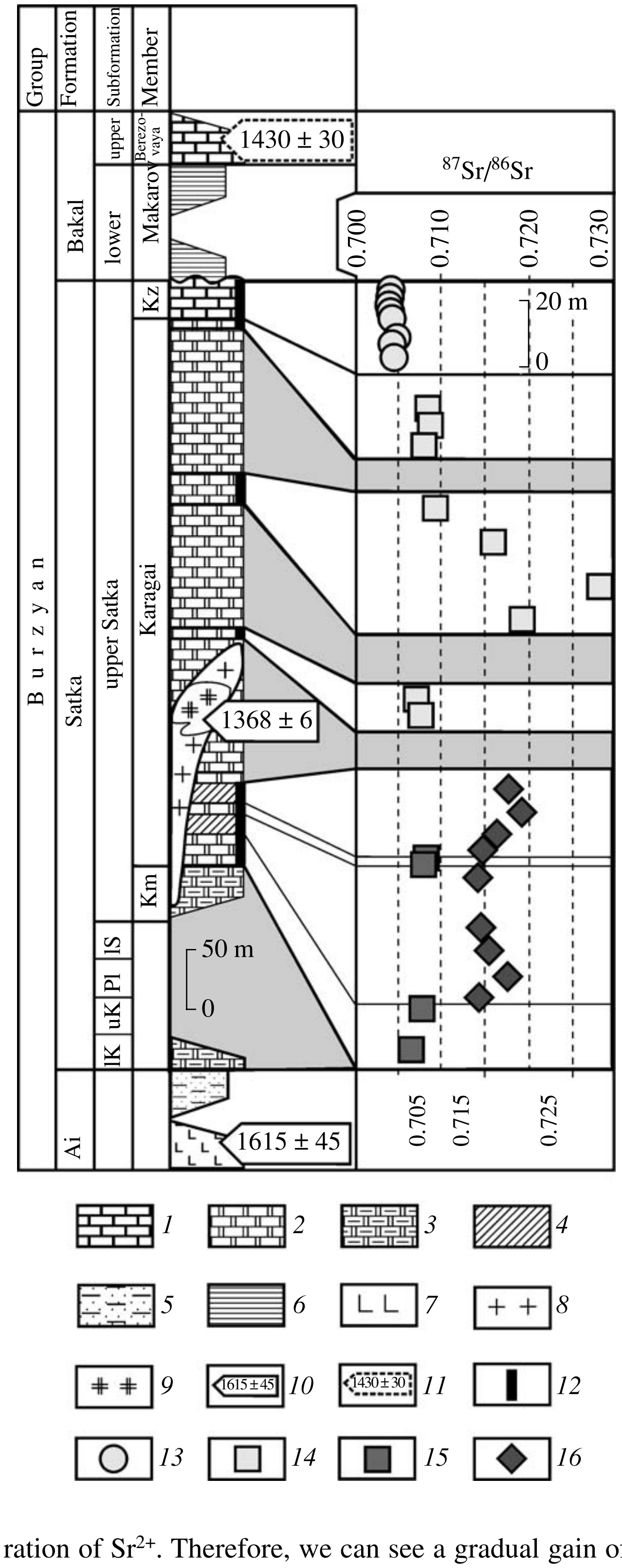

Fig. 2. Structure of the upper part of the Satka Formation, location of samples, and measured $^{87}Sr/^{86}Sr$ ratio. (*1–7*) Rock types: (*1*) limestones, (*2*) dolomites, (*3*) clayey dolomites, (*4*) magnesites, (*5*) siltstones, (*6*) shales, (*7*) volcanic rocks; (*8*) granitic rocks of the Berdyaush pluton; (*9*) nepheline syenites; (*10*) U–Pb zircon age of magmatic rocks (Ma) of the Ai Formation [8] and nepheline syenites of the Berdyaush pluton [10]; (*11*) Pb–Pb age of limestones, Ma [9]; (*12*) interval of sampling; (*13–16*) samples: (*13*) limestones, (*14*) dolomites, (*15*) near-ore dolomites, (*16*) magnesites. Subformations: (lK) lower Kusa; (uK) upper Kusa; (Pl) Polovinka; (lS) lower Satka; members: (Km) Kamennogorka; (Kz) Kyzym, (Mk) Makarov; (Br) Berezovaya.

Rb–Sr analytical data and major element contents in carbonate rocks of the Karagai and Kazym members of the Satka Formation

Sample	Thickness[1], m	Rock[2]	SC[3], %	Mg, %	Ca, %	Rb, ppm	Sr, ppm	$^{87}Rb/^{86}Sr$	$^{87}Sr/^{86}Sr$ meas.	$^{87}Sr/^{86}Sr$ init.[4]
Kazym Member										
UC-79	22	L	3.5	0.1	40.0	0.47	2453	0.0005	0.70473	0.70472
2-21	21	L	0.8	0.2	39.6	0.10	2740	0.0001	0.70465	0.70465
UC-78	20	L	0.9	0.1	40.0	0.03	2753	0.0000	0.70460	0.70460
2-18	19	L	1.7	0.2	39.1	0.12	2180	0.0002	0.70470	0.70470
2-16	15	L	2.2	0.2	39.6	0.12	2340	0.0002	0.70466	0.70466
2-10	9	L	2.9	0.1	39.9	0.19	1140	0.0005	0.70520	0.70519
UC-74	8	L	1.1	0.2	40.0	0.04	1675	0.0001	0.70468	0.70468
UC-73	7	L	3.1	0.1	36.7	0.54	1490	0.0011	0.70482	0.70480
UC-72	5	L	3.3	0.3	36.3	0.58	1180	0.0014	0.70498	0.70495
Karagai Member										
UC-71	640	D	1.3	12.4	21.1	0.07	24.6	0.0083	0.70849	0.70830
2-3	635	D	0.7	12.9	21.6	0.14	66.4	0.0062	0.70900	0.70886
2-1	630	D	2.4	12.8	21.6	0.16	24.8	0.0189	0.70798	0.70756
UC-55	350	D	3.8	13.4	21.0	0.31	47.3	0.0192	0.70936	0.70893
UC-54	340	D	4.7	13.2	21.1	0.13	62.8	0.0061	0.71604	0.71591
UC-53	330	D	15.5	12.7	20.3	0.32	56.4	0.0166	0.73079	0.73042
UC-52	320	D	5.3	12.3	20.0	0.46	46.6	0.0289	0.71932	0.71868
UC-51	210	D	2.3	12.7	20.6	0.06	37.3	0.0048	0.70743	0.70733
UC-50	205	D	1.0	12.5	20.3	0.06	39.3	0.0048	0.70793	0.70783
180-12	92	M	1.3	28.6	0.3	0.25	1.19	0.6087	0.71787	0.71266
180-11	84	M	1.1	27.4	0.8	0.47	3.02	0.4510	0.71935	0.71536
180-10	77	M	1.6	28.1	0.3	0.40	1.68	0.6898	0.71638	0.71028
180-9	71	M	1.9	28.3	0.4	0.31	2.70	0.3326	0.71525	0.71231
180-8	69	NOD	3.4	13.6	21.6	0.50	43.6	0.0336	0.70822	0.70793
180-7	67	NOD	2.7	13.0	21.8	0.44	49.0	0.0263	0.70816	0.70793
180-6	63	M	0.9	28.3	0.3	0.28	1.69	0.4799	0.71425	0.71001
180-5	46	M	1.7	28.5	0.3	0.35	1.07	0.9475	0.71476	0.70639
180-4	38	M	1.5	28.0	0.3	0.38	1.54	0.7148	0.71562	0.70930
180-3	30	M	0.5	28.4	0.5	0.11	4.8	0.0664	0.71793	0.71737
180-1	23	M	1.4	27.8	0.5	0.25	4.0	0.1815	0.71517	0.71357
180-2	20	NOD	2.8	13.0	21.8	0.26	42.6	0.0179	0.70825	0.70809
ST6-45	8	NOD	1.0	–	–	0.30	44.2	0.0199	0.70659	0.70642

Note: (1) Sampling distance from the member base in the summary stratigraphic column; (2) rock type: (L) limestone, (D) dolomite, (NOD) near-ore dolomite; (M) magnesite; (SC) siliciclastic admixture; (4) the initial $^{87}Sr/^{86}Sr$ ratio was calculated at 1550 Ma for distal limestones and dolomites and at 620 Ma for near-ore dolomite and magnesite in line with assumption of the rearrangement of their Rb–Sr systems during the regional listvenitization and potassic alteration.

mites, and magnesites (0.03–0.58, 0.06–0.50, and 0.11–0.47 ppm, respectively). However, because of the extremely low Sr content in magnesites, the Rb/Sr ratio in this rock turns out to be relatively high and the increment of radiogenic ^{87}Sr at the expense of ^{87}Rb decay becomes appreciable. The calculated initial ^{87}Sr/^{86}Sr ratio in magnesites varies from 0.69165 to 0.71663 if we assume that this rock is not younger than 1370 Ma. In this case, the initial ^{87}Sr/^{86}Sr ratio in three samples turns out to be lower than that typical of the mantle reservoir. In one sample, the ratio is even lower than that in the primordial Earth. Hence, the accepted age (1370 Ma) is overestimated and Rb–Sr systems of magnesites and probably other carbonate rocks in the Satka district were rearranged in the process of recrystallization and the input of additional Rb.

The suggested recrystallization could have been coeval with formation of epigenetic dolomite and calcite generations in carbonate rocks and siderites of the Bakal Formation, which was recovered 20 km away from the Satka ore field [9]. In the Bakal ore field, this process was accompanied by development of siderite–ankerite–dolomite–barite veins and local zones of listvenitization and potassic alteration of dolerite dikes that crosscut the Bakal Formation [6]. The K–Ar age of fuchsites and potassium feldspars from aureoles of diabase dikes is 610–618 Ma [15] and corresponds to the regional tectonothermal activation at the Late Riphean–Vendian boundary. Thus, we can suggest that disturbance of the Rb–Sr system of magnesites and dolomites in the Satka ore field was provoked by potassic metasomatism about 620 Ma ago.

Taking the age of the last event into consideration, the initial ^{87}Sr/^{86}Sr ratio of magnesites and near-ore dolomites is estimated at 0.70639–0.71737 and 0.70642–0.70809, respectively. The coincidence of the minimum values of the initial ^{87}Sr/^{86}Sr ratio in various groups of carbonate rocks is consistent with the replacement of dolomites by magnesites [1, 7]. However, the high ^{87}Sr/^{86}Sr ratio in most samples of the Satka magnesite cannot be attributed exclusively to the in-situ decay of ^{87}Rb and the consequent enrichment in radiogenic ^{87}Sr, as was suggested by Frimmel [5] for magnesites in the Sunk ore field in the Alps. The reaction of the carbonate component with the associated siliciclastic admixture suggested for distal dolomites also does not explain adequately the high ^{87}Sr/^{86}Sr ratio in magnesites, because the contribution of this admixture is very low (0.5–1.9%). Furthermore, in contrast to dolomites, the Rb content and ^{87}Sr/^{86}Sr ratio in the carbonate component of magnesites do not correlate with the amount of silicate material therein. Hence, the high ^{87}Sr/^{86}Sr ratio in magnesites and its gradual increase in the near-ore dolomites indicate that Mg-bearing solutions were enriched in radiogenic ^{87}Sr beyond the limits of host carbonate rocks. These solutions probably assimilated Mn, Fe, and radiogenic ^{87}Sr during their migration through siliciclastic rocks.

The Sr isotope characteristics suggest that limestones of the Satka Formation were deposited in a marine basin connected with the Early Riphean ocean, whereas the Satka dolomites and magnesites could not be deposited simultaneously in sabkhas and lagoons, which were partly isolated from the Early Riphean ocean. However, the dolomites and magnesites could hardly be formed in a closed system during the early diagenetic transformation of carbonate sediments with the participation of connate seawater. The ^{87}Sr/^{86}Sr ratio in limestones shows a significant difference (0.70460–0.70472). Moreover, the ^{87}Sr/^{86}Sr value is minimal in dolomites of the upper Satka subformation (0.70733–0.70783 in distal zones, 0.70642–0.70809 near orebodies). These facts indicate that carbonate sediments were dolomitized in a medium with isotopic signatures distinct from those of the Early Riphean seawater. Magnesites were produced by the metasomatic replacement of dolomites with the participation of ^{87}Sr-rich solutions in the process of their interaction with siliciclastic rocks and minerals. This conclusion does not contradict the infiltration-brine and hydrothermal metasomatic models of the genesis of stratiform magnesites in the Satka Formation.

ACKNOWLEDGMENTS

This work was carried out within the framework of the Program of the Division of Earth Sciences, Russian Academy of Sciences ("Isotopic Systems and Isotopic Fractionation in Natural Processes") and supported by the Russian Foundation for Basic Research (project nos. 04-05-65124 and 06-05-64592).

REFERENCES

1. L. V. Anfimov, B. D. Busygin, and L. E. Demina, *The Satka Magnesite Deposit in the Southern Urals* (Nauka, Moscow, 1983) [in Russian].
2. P. P. Smolin, A.I, Shevelev, L. P. Urasina, et al., *Genetic Types, Localization, and Forecast of Brucite and Magnesite Deposits* (Nauka, Moscow, 1984) [in Russian].
3. W. Pohl and W. Siegl, in *Handbook of Stratiform and Stratabound Ore Deposits* (Elsevier, Amsterdam, 1986), pp. 223–310.
4. H. E. E. Frimmel and G. Niedermeyer, Appl. Geochem. **6** (1), 89 (1991).
5. H. E. E. Frimmel, Miner. Deposita **23** (4), 268 (1988).
6. A. V. Maslov, M. T. Krupenin, E. Z. Gareev, and L. V. Anfimov, *The Riphean on the Western Slope of the Southern Urals: Classic Sections, Sedimentation, Lithogenesis, Minerageny, and Geological Natural Monuments* (Inst. Geol. Geokhim., Yekaterinburg, 2001), Vol. 1 [in Russian].

7. M. T. Krupenin, Dokl. Earth Sci. **405**, 1256 (2005) [Dokl. Akad. Nauk **405**, 243 (2005)].
8. A. A. Krasnobaev, E. V. Bibikova, Yu. L. Ronkin, et al., Izv. Ross. Akad. Nauk, Ser. Geol., No. 6, 25 (1992).
9. A. B. Kuznetsov, M. T. Krupenin, G. V. Ovchinnikova, et al., Lithol. Mineral. Res. **40**, 195 (2005) [Litol. Polezn. Iskop **40**, 227 (2005)].
10. Yu. L. Ronkin, D. I. Matukov, S. L. Presnyakov, et al., Litosfera, No. 1, 135 (2005).
11. A. N. Zavaritsky, Gornoe Delo, No. 2/3, 37 (1920).
12. M. T. Krupenin and V. Prochaska, Dokl. Earth Sci. **403A**, 833 (2005) [Dokl. Akad. Nauk **403**, 661 (2005)].
13. I. M. Gorokhov, M. A. Semikhatov, A. V. Baskakov, et al., Stratigr. Geol. Korrel. **3** (1), 3 (1995).
14. I. M. Gorokhov, A. B. Kuznetsov, V. A. Melezhik, et al., Dokl. Earth Sci. **360**, 609 (1998) [Dokl. Akad. Nauk **360**, 533 (1998)].
15. M. A. Garris, *Stages of Magmatism and Metamorphism in the Pre-Jurassic History of the Urals and Fore-Urals* (Nauka, Moscow, 1977).